Electronic Supplementary Information (ESI):

Nanoscale fracture of defective popgraphene monolayer

Fanchao Meng[1], Ming Ni[1], Feng Chen[1], Jun Song[2*], Dong Wei[1*]

1. BGI-Shenzhen, Shenzhen 518083, China
2. Department of Mining and Materials Engineering, McGill University, Montreal, Quebec H3A 0C5, Canada

S1 Effects of temperature and strain rate on the stress-strain response of popgraphene

The results presented in this study were obtained using a temperature of 1 K and a strain rate of 1×10^{-3} ps^{-1}. In general, a higher temperature will introduce higher thermal energy to the material system and result in lower fracture stress (with and without defects), as demonstrated in the work of, e.g., Dewapriya et al.[1] and Zhao and Aluru.[2] For popgraphene, we also examined a few high temperatures including 300 K, 600 K, 900 K, and 1200 K using popgraphene with a nanocrack ($a = 27.94$ Å) loaded normal to the ZZ direction as a representative case, as shown in **Fig. S1a**. We found a similar conclusion with previous studies.

Higher strain rate usually results in higher fracture stress than that of lower strain rate. However, comparing with temperature, previous studies have demonstrated that the effect of strain rate is less significant (for strain rate of 10^9/s, 10^8/s, and 10^7/s).[2, 3] To confirm the above, we performed additional simulations using different strain rates on the same models that we used for testing the temperature effect, as shown in **Fig. S1b**, and found a similar conclusion with previous studies.

* Corresponding authors. E-mail: jun.song2@mcgill.ca (Jun Song); weidong@genomics.cn (Dong Wei)

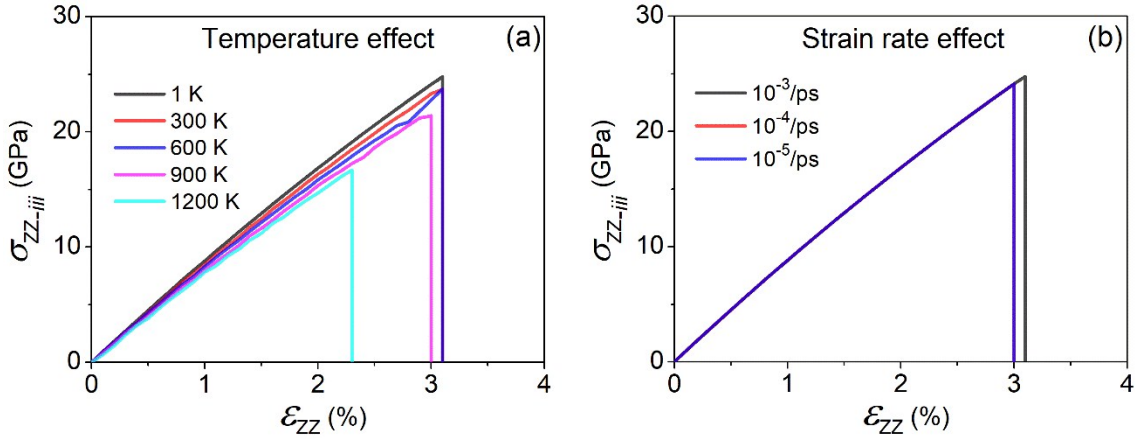

Figure S1. Stress-strain curves of popgraphene with a nanocrack of crack size $a = 27.94$ Å loaded normal to the ZZ direction under (a) different temperatures and (b) different strain rates.

S2 Independence of fracture stress on the initial degree of crumpling

As stated in **Section 3.3** of the main text, the fracture stress of popgraphene loaded at 1 K is independent of the initial degree of crumpling. To support the above statement, we performed two sets of studies for popgraphene with distributed SV defects using NPT ensemble: *i)* popgraphene was equilibrated at T=1 K, followed by uniaxial tension at T=1 K; *ii)* popgraphene was equilibrated at T=300 K, followed by uniaxial tension at T=1 K, which will promote overall larger crumpling amplitude. Defect densities ranging from 0.25% to 1.0% were considered, and the stress-strain curves of the above were shown in **Fig. S2**, where we see negligible variations in the fracture stresses (i.e., the maximal stress from the stress-strain curve) of the comparison pair. Therefore, we conclude that the fracture stress is mostly determined by the loading conditions, while being insensitive to the initial degree of crumpling.

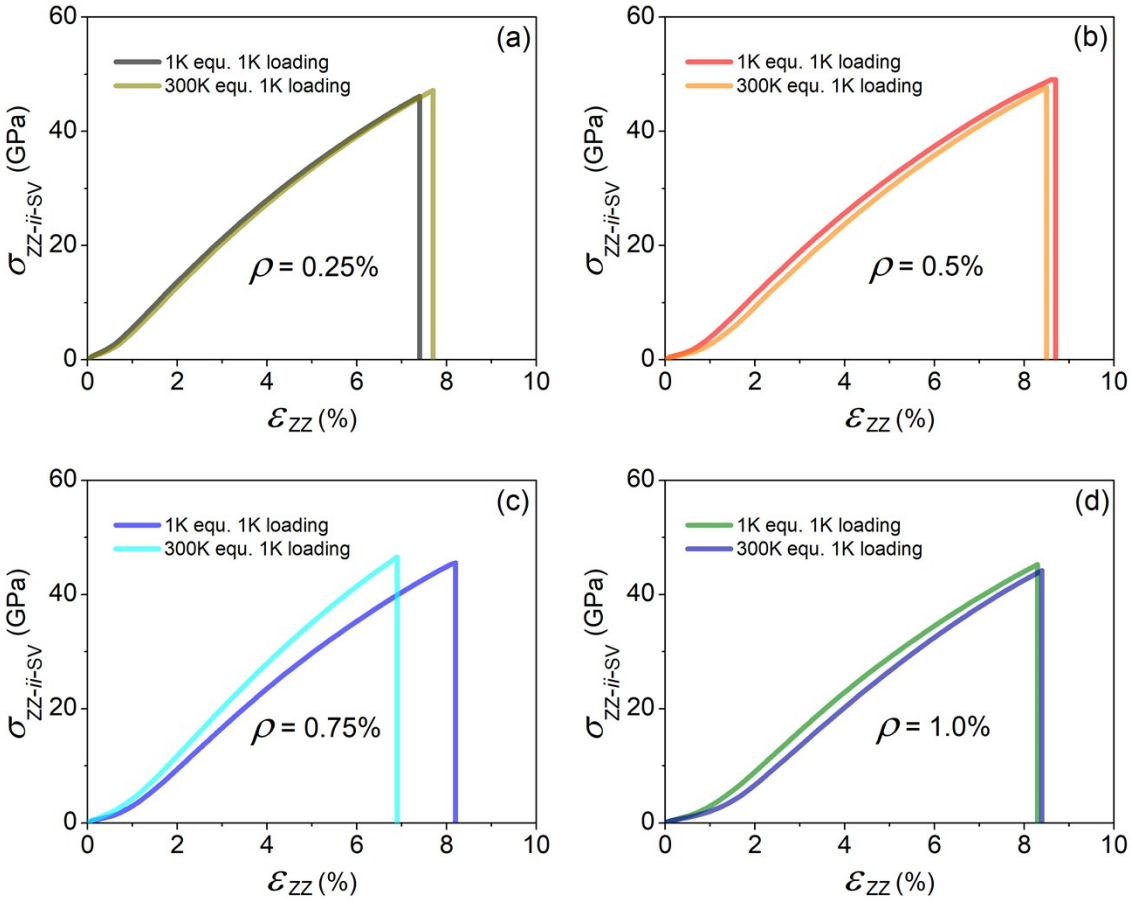

Figure S2. Stress-strain curves of popgraphene with distributed point defects uniaxially loaded normal to the ZZ direction of defect densities (a) $\rho = 0.25\%$, (b) $\rho = 0.5\%$, (c) $\rho = 0.75\%$, and (d) $\rho = 1.0\%$.

S3 Insensitive of the overall stress-strain response of popgraphene to crumpling

Based on Wei et al.'s work[4] and our results, crumpling can be eliminated by an elastic strain. Therefore, we expect that crumping will not evidently contribute to the overall stress-strain response of defective popgraphene. Nevertheless, crumpling will add compliance to the popgraphene sheet and it is expected that with crumpling the stress will be smaller (comparing at the same strain) while fracture strain will be larger than that without crumpling.

To support the above statement, we performed calculations for defective popgraphene confined within the two-dimensional plane (i.e., no crumpling), and plotted the stress-strain curve together with that with crumpling for a range of defect densities (uniaxial load normal to the zigzag direction and single vacancy were used for demonstration), as shown in **Fig. S3**. We see that before fracture, overall, the stress is smaller for popgraphene with crumpling than that without crumpling at the same strain, and the fracture strain is always large when crumping is present, which become more significant when defect density (i.e., the degree of crumpling) is large. These observations are in agreement with our speculations above.

To quantify how much the crumpling contribute to the stress-strain curve, we compared the strain energy of the two scenarios, as listed in **Tab. S1**, where we find that the relative increment of strain energy is generally small, albeit exhibiting certain variations. Therefore, we conclude that crumpling has a negligible effect on the overall stress-strain response of popgraphene.

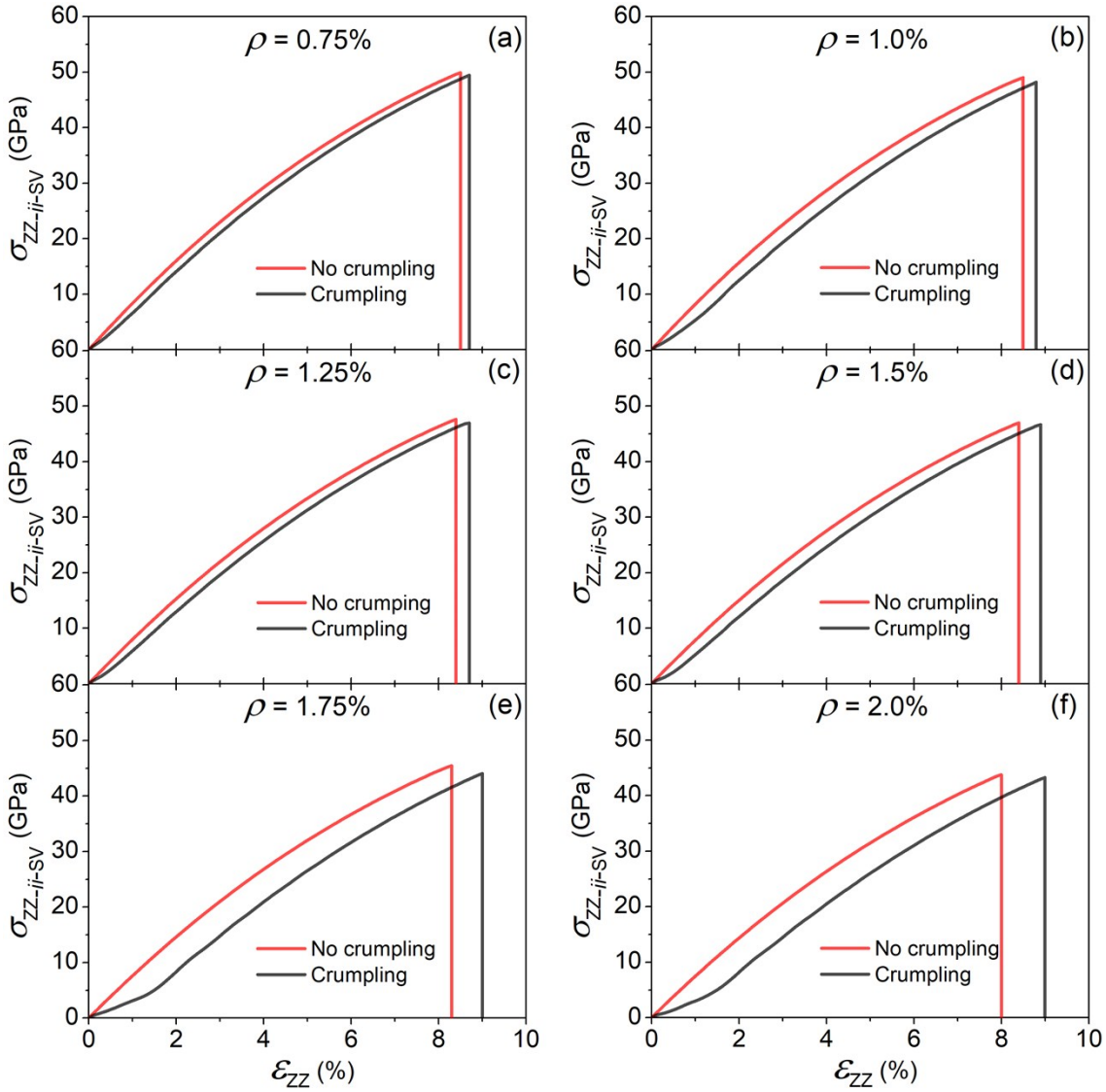

Figure S3. Stress-strain curves of defective popgraphene with (black lines) and without (red lines) crumpling for defect density ranging from $\rho = 0.75\%$ to $\rho = 2.0\%$ from (a) to (f). Loading is uniaxial and normal to the ZZ direction. The single vacancy was used to generate the crumpling.

Table S1. Strain energy of defective popgraphene with and without crumpling for a range of defect densities from 0.75% to 2.0%, and the relative increment of strain energy calculated from popgraphene with crumpling to without crumpling

Strain energy (GPa) / Defect density	Crumpling	No crumpling	**Relative increment in strain energy**
0.75%	2.41	2.44	**1.2%**
1.0%	2.32	2.40	**3.4%**
1.25%	2.27	2.29	**0.9%**
1.5%	2.28	2.26	**-0.9%**
1.75%	2.04	2.16	**5.9%**
2.0%	2.00	1.99	**-0.5%**

However, we note that at very small defect density, e.g., $\rho = 0.25\%$ and $\rho = 0.5\%$, popgraphene without crumpling possesses both higher fracture stress and higher fracture strain, as shown in **Fig. S4a-b**. We examined the atomic configuration during loading at both defect densities, and found that local structural reconstruction occurs around the defect for popgraphene without crumpling (highlighted using black ellipses in **Fig. S4c** using $\rho = 0.25\%$ as a representation), which results in the higher stress and strain in the structure without crumpling.

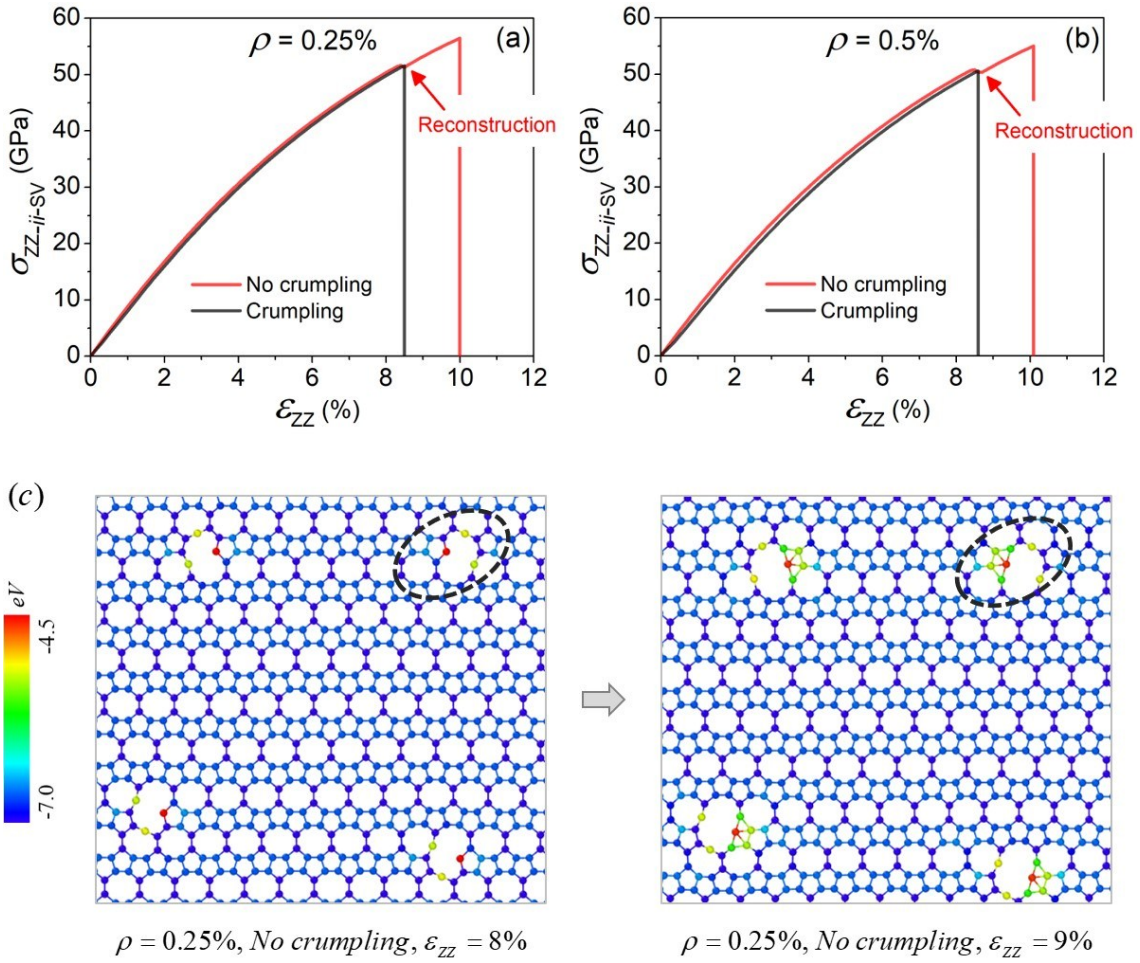

Figure S4. Stress-strain curves of defective popgraphene with (black lines) and without (red lines) crumpling for defect density ranging from $\rho = 0.25\%$ to $\rho = 0.5\%$ from (a) to (b). (c) shows the atomic configurations of popgraphene without crumpling loaded at 8% and 9% strains at the defect density of $\rho = 0.25\%$. Atoms are colored according to potential energy contour with a scale bar from -7.0 to -4.5 eV. The representative place where structural reconstruction occurred was enclosed by black ellipses.

S4 Origin of the large reduction and variation of fracture stress of popgraphene with distributed SW defects

As stated in **Section 3.3** of the main text, we observed large reduction and variation of the fracture stress for popgraphene with distributed SW defects, particularly at large defect densities. To understand the above phenomena, we looked into the relaxed supercells with SW defects before loading, as shown in **Fig. S5**, and found that there exists high prestress localization in atoms around the SW transformation. Such stress localization will further promote out-of-plane crumpling upon relaxation and easily render random loss of atoms from the popgraphene sheet, especially at large defect densities. Therefore, we conclude that the above phenomena could be attributed to the large prestress localization of the SW defects.

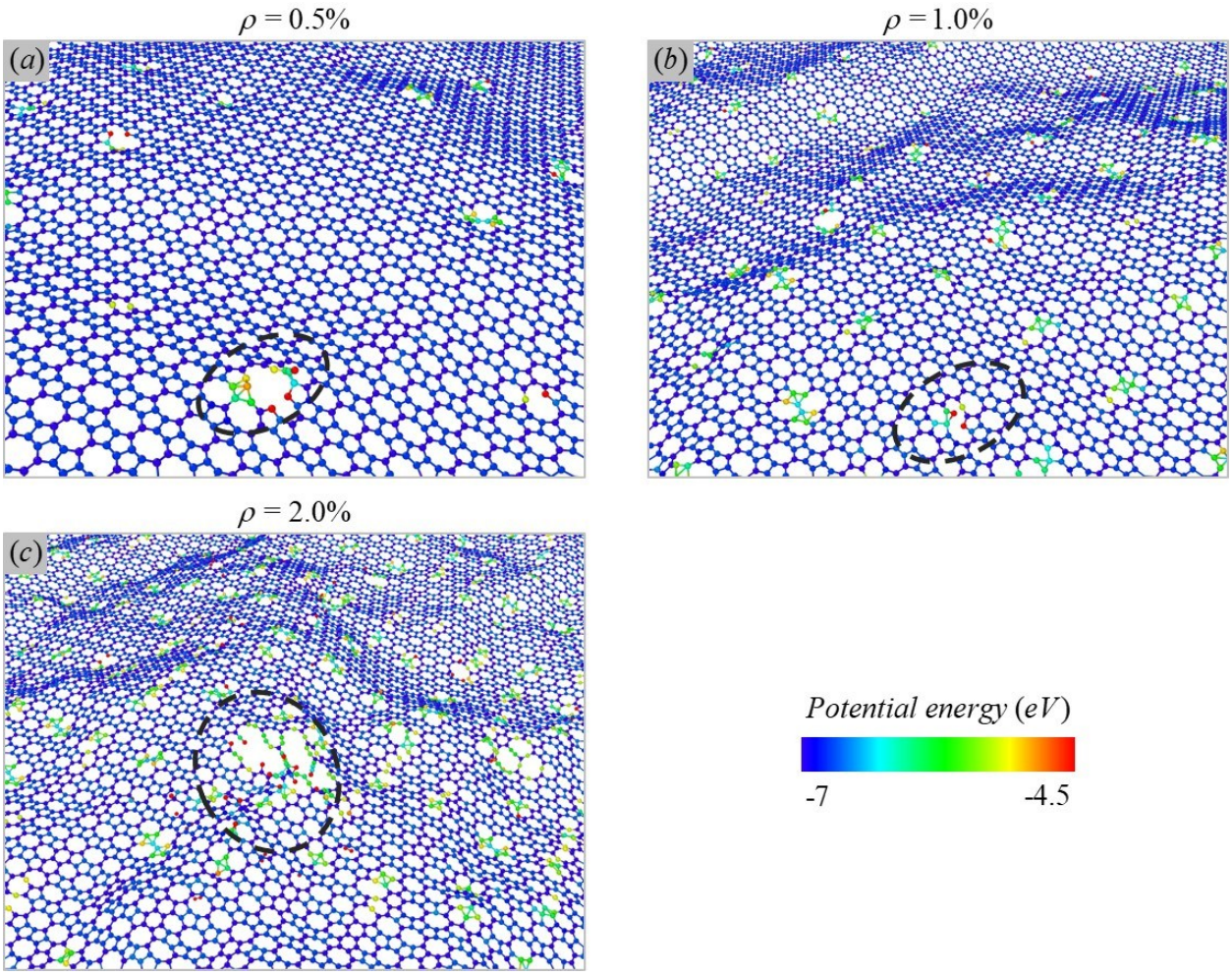

Figure S5. Partial sheets within representative defective popgraphene containing distributed SW defects of defect densities (a) $\rho = 0.5\%$, (b) $\rho = 1.0\%$, and (c) $\rho = 2.0\%$ after relaxation at 1 K. showing crumpling throughout the sheet. Atoms are colored according to potential energy contour with a scale bar from -7.0 to -4.5 eV. Regions enclosed by the dashed ellipse were places that having high prestresses and/or prestress induced loss of atoms.

S5 Rational for using tangent modulus in Griffith's criterion

As stated in **Section 3.4** of the main text, we referred to Dewapriya et al.'s study[1] to use tangent modulus in Griffith's criterion in order to correctly reflect the nonlinear stress-strain

response of popgraphene. The tangent modulus of popgraphene E_t was obtained by fitting the stress-strain curves of popgraphene at each corresponding crack size using a second-order polynomial function and subsequently plug in the fracture strain into the first derivative of the polynomial function. The stress-strain curves of popgraphene with ZZ and AC cracks as functions of crack size a were plotted in **Fig. S6a-b**, respectively, and the corresponding tangent modulus of the above two situations were plotted in **Fig. S6c-d**, respectively.

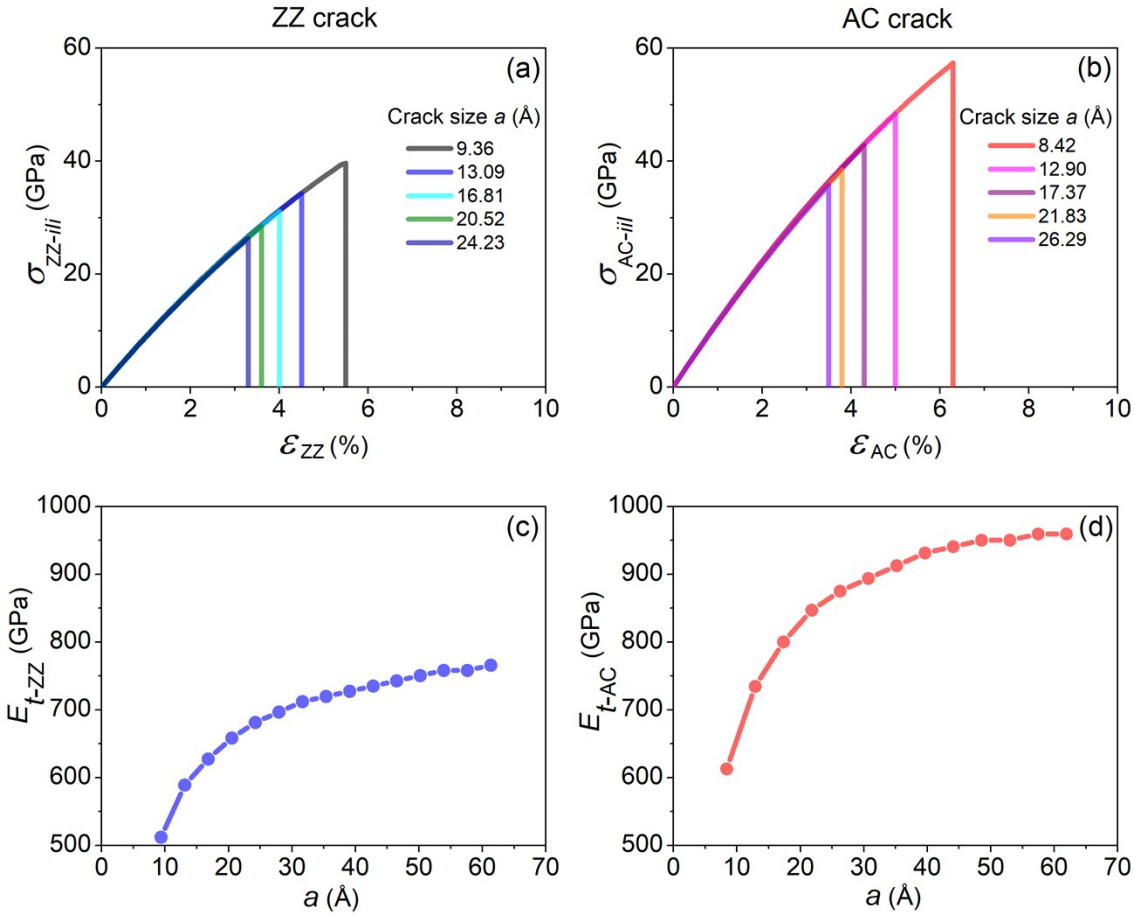

Figure S6. Sample simulated fracture stresses as functions of the crack size a of (a) ZZ and (b) AC cracks, respectively. (c) and (d) plot the tangent modulus E_t as functions of crack size a for ZZ and AC cracks, respectively.

S6 Insensitive of the fracture of popgraphene to atomic structures of the crack tip

In the main text, we only considered cracks terminated at the junction or side of the 8-ring as shown in **Fig. 4a-b** of the main text. Nevertheless, based on the results of the "8-ring" crack tip, Griffith criterion holds for popgraphene, i.e., the facture is governed by an energy criterion and determined by the associated fracture energy. Therefore, we expect the result will not be sensitive to the local bond at the crack tip.

To verify the above judgment, we created cracks of different crack sizes that end at the sides or the junction of the 5-rings as shown in **Fig. S7a** and **S7c**. The fracture stresses as functions of crack size for both cracks were plotted in **Fig. S7b** and **S7d** respectively, where, in general, nice coincidence of the fracture stress with those calculated from the crack created at the sides or the junction of 8-ring.

However, we noticed that for cracks end at the side of 5-ring the fracture stress is smaller than that of 8-ring at small crack sizes. The possible reason is that the critical bond of the former is parallel, while that of the latter is oblique to the loading direction, the effect of which may be more obvious at the small crack size. In addition, for cracks end at the junction of 5-ring, the fracture stress is overall larger than that of 8-ring due to the local structural reconstruction of the former. Nevertheless, overall, the fracture stress is not sensitive to the atomic structure of the crack tip.

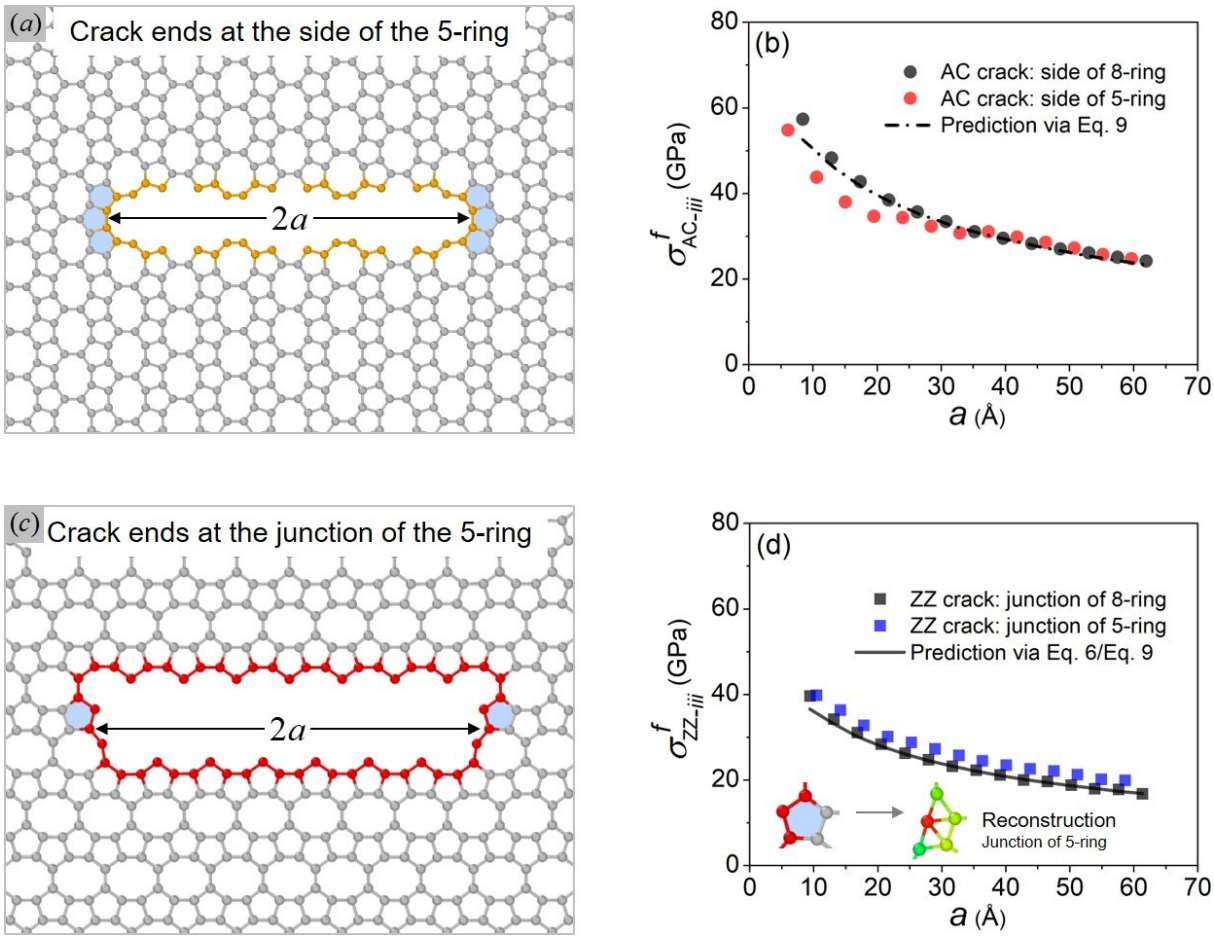

Figure S7. Atomistic configurations of the popgraphene monolayer with crack tips end at the (a) side and (c) junction of the 5-ring. The internal crack size is denoted as $2a$. (b) and (d) plot the simulated and predicted fracture stresses as functions of the crack size a for cracks in (a) and (c), respectively, together with cracks with crack tips end at the side or the junction of the 8-ring reported in the main text. The inset in (d) shows the structural reconstruction at the crack tip for crack ends at the junction of 5-ring.

REFERENCES (ESI)

1. M. Dewapriya, R. Rajapakse and A. Phani, *Int. J. Fract.*, 2014, **187**, 199-212.

2. H. Zhao, K. Min and N. Aluru, *Nano Lett.*, 2009, **9**, 3012-3015.

3. F. Meng, C. Chen and J. Song, *Carbon*, 2017, **116**, 33-39.

4. Y. Wei, J. Wu, H. Yin, X. Shi, R. Yang and M. Dresselhaus, *Nat. Mater.*, 2012, **11**, 759-763.